

# EAGLE-360: Embodied Active Global-to-Local Exploration in 360°

Jingtao Xu<sup>1</sup>, Zizhuo Lin<sup>1</sup>, Jianwen Sun<sup>2</sup>, Yi Yang<sup>1</sup>, Yawei Luo<sup>1\*</sup>

<sup>1</sup>Zhejiang University

<sup>2</sup>Central China Normal University

<https://github.com/Sansju/EAGLE-360>

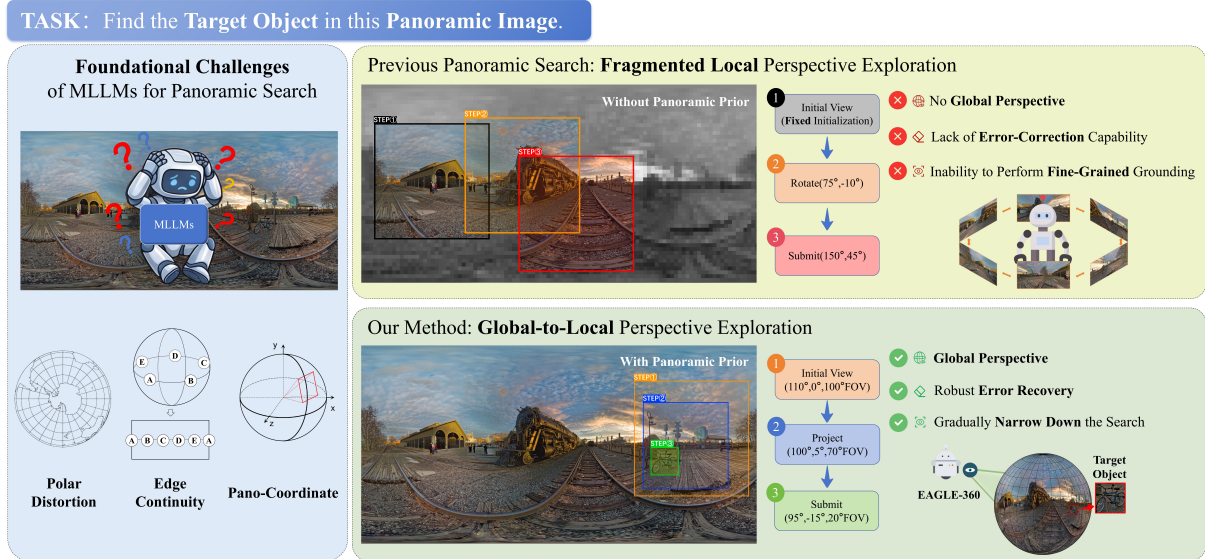


Figure 1: **Overview of Target Object Search in Panoramic Images.** **Left:** Conventional MLLMs struggle with inherent 360° properties, such as polar distortion and edge continuity. **Top Right:** Previous panoramic search methods rely on fragmented local exploration. Burdened by fixed initialization and rigid rotations without a panoramic prior, they suffer from poor error recovery and lack fine-grained grounding capabilities. **Bottom Right:** Our proposed framework introduces an active *global-to-local* perspective exploration strategy. By leveraging a panoramic prior, it dynamically adjusts the Field of View (FOV) to progressively narrow down the search space, enabling robust error recovery and precise target grounding.

## Abstract

While Multimodal Large Language Models (MLLMs) have demonstrated exceptional capabilities in standard visual understanding, adapting them for active visual search in 360° panoramic environments exposes fundamental limitations. Specifically, standard MLLMs struggle to effectively model inherent panoramic properties—such as severe polar distortion and continuous cylindrical topologies—which significantly degrades target detection accuracy. Consequently, existing panoramic search methods attempt to compensate by relying heavily on fragmented local viewpoints. Burdened by rigid initialization and a lack of global panoramic priors, these approaches suffer from myopic, inefficient explo-

ration and struggle with robust error recovery when targets are out of view. To overcome these challenges, we propose **EAGLE-360**, a novel Embodied Active Global-to-Local Exploration framework. Rather than performing exhaustive local searches, EAGLE-360 leverages global priors to establish an initial holistic perspective, iteratively reasoning and progressively narrowing the search space. Architecturally, we adapt RoPE Rolling—a coordinate-shifting positional encoding mechanism—to seamlessly model the continuous topologies of panoramas. To facilitate this paradigm, we construct the large-scale EAGLE-360 dataset, comprising 14,000+ 4K panoramas and 70,000+ rounds of high-quality VQA dialogues. By employing a training pipeline that integrates Supervised Fine-Tuning (SFT) with Group Relative Policy Optimization (GRPO), we effectively elicit

\* Corresponding author.

complex spatial reasoning and tool-calling capabilities. Extensive experiments demonstrate that EAGLE-360 establishes a new state-of-the-art for 360° visual search, achieving nearly an 8-fold increase in accuracy over the base model while significantly enhancing exploration efficiency.

## 1 Introduction

Active visual search is a core capability of embodied intelligence, requiring agents to progressively accumulate evidence to localize a target. While Multimodal Large Language Models (MLLMs) have substantially advanced instruction-following and grounded navigation (Qi et al., 2020; Ramakrishna et al., 2022; Khanna et al., 2024; Yokoyama et al., 2024; Zhou et al., 2024; Zheng et al., 2024; Zhang et al., 2024), current paradigms remain constrained by egocentric, localized perspectives. Integrating 360° panoramas offers a principled, holistic alternative that mitigates viewpoint initialization biases. However, directly applying standard MLLMs to equirectangular projections exposes three fundamental architectural and perceptual limitations: severe vulnerability to polar distortion, the disruption of continuous edge topologies at artificial boundaries, and an inherent inability to perform panocoordinate modeling in a 3D spherical space.

Constrained by these foundational architectural deficits, prior panoramic methods (Yu et al., 2025) suffer from a critical procedural failure: short-sighted search. By relying on fragmented local perspective crops and rigid iterative adjustments from a localized initial view, they exhibit myopic reasoning and frequently fail when targets lie outside the starting Field of View (FoV). Furthermore, while previous literature highlights these geometric challenges (Chou et al., 2020a; Yun et al., 2021; Zhang et al., 2025b; Dongfang et al., 2025; Zhou et al., 2025) and advocates for spherical inductive biases (Ling et al., 2023; Benny and Wolf, 2025; Ren et al., 2025), most work remains limited to passive understanding tasks (Chou et al., 2020c; Yun et al., 2021; Zhang et al., 2025b; Dongfang et al., 2025; Zhou et al., 2025). We argue that active visual search in panoramas must fundamentally be framed as a global-to-local problem—requiring the agent to first reason over the holistic scene layout before progressively narrowing its attention to a target-centered local region.

To this end, we propose **EAGLE-360**, an Embodied Active Global-to-Local Exploration frame-

work for autonomous panoramic object search. Eschewing arbitrary local initialization, our agent leverages the complete 360° panorama to estimate the target’s rough angular region. It then executes a tool-augmented iterative exploration, repeatedly invoking an equirectangular-to-perspective projection tool to manipulate azimuth, elevation, and FoV until the target is precisely localized within a spherical Bounding Field of View (BFoV). Crucially, EAGLE-360 employs RoPE Rolling (Ren et al., 2025) for panorama-aware positional modeling. This seamlessly models the continuous cylindrical wrap-around topology, inherently overcoming the topological constraints of standard MLLMs.

To support this paradigm, we construct the EAGLE-360 dataset, comprising over 14,000 4K panoramas and 70,000+ rounds of search-oriented Chain-of-Thought (CoT) trajectories. We design a robust two-stage training pipeline: Supervised Fine-Tuning (SFT) to establish the basic action space, followed by Group Relative Policy Optimization (GRPO) to align the exploration strategy. By reinforcing successful trajectory outcomes, GRPO effectively stabilizes multi-step tool invocation in ultra-long contexts.

Extensive experiments demonstrate that our model achieves state-of-the-art (SOTA) performance on the EAGLE-360 dataset (64.44% accuracy—a nearly 8-fold improvement over the base model—with a Great Circle Distance error of just 16.89°). Furthermore, EAGLE-360 exhibits exceptional zero-shot transferability, achieving a score of 56.1 on the out-of-distribution H\*Bench, significantly outperforming both leading open-source and proprietary models.

**Contributions.** (1) We redefine panoramic active visual search as a holistic 360° global-to-local exploration task, overcoming the procedural failures of short-sighted, localized initializations. (2) We propose EAGLE-360, an embodied framework that integrates RoPE Rolling to mitigate foundational MLLM architectural flaws, utilizing tool-augmented reasoning for precise spherical BFoV localization. (3) We introduce the large-scale EAGLE-360 dataset, featuring over 80,000 detailed CoT reasoning trajectories tailored for panoramic search. (4) We implement an SFT and GRPO training pipeline that yields unprecedented SOTA performance on our benchmark and exceptional zero-shot transfer capabilities on H\*Bench.

## 2 Related Work

### 2.1 Embodied Visual Search and Navigation

Embodied agents must seamlessly integrate perception, language, and action. Early benchmarks established foundational tasks for indoor navigation and remote object grounding (Qi et al., 2020; Ramakrishna et al., 2022; Khanna et al., 2024; Yokoyama et al., 2024). Recently, MLLM-based agents have leveraged foundation models for explicit reasoning and historical context modeling in navigation policies (Zhou et al., 2024; Zheng et al., 2024; Zhang et al., 2024; Zhu et al., 2025; Zhang et al., 2025a). While these approaches demonstrate strong performance on egocentric views or top-down maps, achieving comprehensive spatial awareness in unconstrained environments remains an open challenge, as localized initial views often necessitate complex procedural steps to capture the full scene. Closest to our setting, *Thinking in 360°* (Yu et al., 2025) and ReasonNavi (Ao et al., 2026) explore panoramic and global-first reasoning. Building upon these insights, EAGLE-360 introduces a holistic *global-to-local* exploration paradigm: it utilizes the complete panorama upfront to provide a broader spatial context, facilitating the prediction of a spherical bounding field of view (BFoV) through deliberate, multi-turn refinement.

### 2.2 Omnidirectional Vision-Language Understanding

Adapting standard MLLMs to the unique properties of omnidirectional imagery presents distinct challenges. Early efforts primarily focused on basic 360° VQA and spatial grounding (Chou et al., 2020b; Cirik et al., 2020; Yun et al., 2021; Chou et al., 2020c). Recently, a surge of comprehensive benchmarks—including OSR-Bench, 360-R1, and Dense360 (Dongfang et al., 2025; Zhang et al., 2025b; Zhou et al., 2025; Yang et al., 2025; Tran et al., 2026; Lin and Zheng, 2026; Chen et al., 2025)—has further highlighted the complexities of panoramic spatial reasoning. These works provide valuable insights into *passive* understanding tasks, such as dense captioning and single-turn QA. Complementing these passive evaluation settings, there is a growing need to explore active, sequential decision-making within panoramas. Our framework addresses this open area by requiring the model to estimate global directions, dynamically invoke projection tools, and iteratively refine its spatial belief for precise object localization.

### 2.3 Panorama-Aware Geometry Modeling

Equirectangular projections (ERP) introduce specific architectural considerations, such as polar distortion and edge discontinuity. To accommodate these geometric properties, prior methods have successfully incorporated inductive biases via horizontal structures (Sun et al., 2019, 2021), spherical networks (Cohen et al., 2018; Ling et al., 2023; Benny and Wolf, 2025), and adapted positional encodings like RoPE Rolling (Ren et al., 2025). For active embodied agents, accurate pano-coordinate modeling and edge continuity extend beyond static feature learning; they also play a crucial role in continuous action planning. Seamless spatial representations are essential to ensure agents can naturally track and locate objects across artificial image boundaries. By integrating modality-aligned RoPE Rolling, EAGLE-360 aligns with this geometry-aware direction, facilitating smooth and uninterrupted exploration across the spherical domain.

## 3 Method

We present EAGLE-360 (Embodied Active Global-to-Local Exploration in 360°), a multimodal framework for autonomous panoramic object search. Unlike previous methods relying on heavily constrained viewpoint priors, EAGLE-360 directly processes the unconstrained panorama. As illustrated in Figure 2, it employs a progressive exploration paradigm, seamlessly transitioning from holistic scene perception to precise local refinement.

### 3.1 Problem Formulation

We model the autonomous panoramic search as a Partially Observable Markov Decision Process (POMDP). At episode start ( $t = 0$ ), the agent receives a full equirectangular panorama  $I_{\text{pano}} \in \mathbb{R}^{H \times W \times 3}$  and a natural language query  $Q$ .

Since mapping planar bounding boxes to equirectangular images introduces severe polar distortion, we define the localization target natively on the unit sphere as a Bounding Field of View (BFoV):

$$\mathcal{B} = (\theta_c, \phi_c, f_h, f_v), \quad (1)$$

where  $\theta_c \in [-\pi, \pi)$  and  $\phi_c \in [-\frac{\pi}{2}, \frac{\pi}{2}]$  represent the azimuth and elevation of the view center, and  $f_h, f_v$  denote the horizontal and vertical Field of View (FoV) extents.

The agent predicts a final  $\mathcal{B}^*$ . A success is registered if the great-circle distance between the predicted center  $(\theta_c^*, \phi_c^*)$  and the ground-truth center

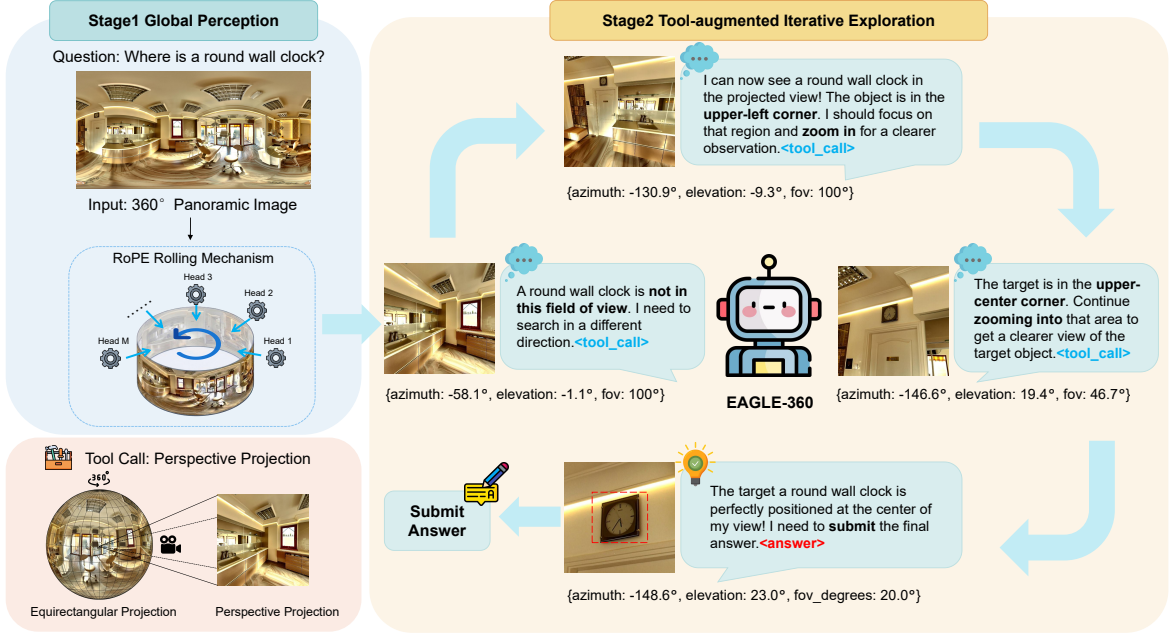


Figure 2: **The overall pipeline of the proposed EAGLE-360 framework.** Our method adopts an embodied active exploration paradigm that transitions from a global panorama to a precise local view. Stage 1: Global Perception processes the input 360° panoramic image utilizing a novel RoPE Rolling Mechanism. This mechanism explicitly addresses the left-right boundary continuity issue, enabling the model to effectively understand the rotational consistency of panoramas and establish a comprehensive global field of view. Stage 2: Tool-augmented Iterative Exploration simulates active observation by invoking a Perspective Projection tool. Guided by the global context, the model iteratively reasons and dynamically adjusts camera parameters (azimuth, elevation, and FOV) to navigate the environment. This coarse-to-fine process continuously narrows the search space until the target object is precisely located and the final answer is submitted.

$(\theta_{gt}, \phi_{gt})$  is within half the ground-truth bounding-box diagonal angle,  $\delta_{\text{bbox}}$ :

$$d_{gc}((\theta_c^*, \phi_c^*), (\theta_{gt}, \phi_{gt})) \leq \frac{1}{2} \delta_{\text{bbox}}. \quad (2)$$

This spherical formulation eliminates projection artifacts, ensuring a spatially rigorous evaluation criterion.

### 3.2 Global-to-Local Exploration Framework

To localize objects accurately, EAGLE-360 executes a unified global-to-local search pipeline, tightly coupling initial spatial reasoning with iterative visual refinement.

**Global Perception via RoPE Rolling.** The agent first evaluates the complete 360° context to identify the target’s coarse direction. A fundamental challenge in equirectangular projection is the *seam discontinuity*: standard 2D Rotary Position Embeddings (RoPE) treat the left ( $x = 0$ ) and right ( $x = W - 1$ ) boundaries as maximally distant, despite their physical adjacency on the sphere.

To guarantee topologically consistent perception within the MLLM backbone, we introduce

a RoPE Rolling Mechanism. For an input feature map  $\mathbf{X} \in \mathbb{R}^{H \times W \times C}$  and  $N_h$  attention heads, we assign a head-specific horizontal offset  $\Delta n_k$  to the  $k$ -th head:

$$\Delta n_k = \left\lfloor \frac{k}{N_h} \cdot W \right\rfloor. \quad (3)$$

The rolled horizontal coordinate for a spatial position  $(m, n)$  becomes:

$$n'_k = (n + \Delta n_k) \bmod W. \quad (4)$$

By applying these updated coordinates  $R_{\Theta}(m, n'_k)$  to the query and key vectors, different attention heads process the panorama under shifted rotational frames. Consequently, every vertical column serves as a centered context at least once. This enables seamless feature correlation across the left-right boundary without introducing additional network parameters.

**Local Refinement via Iterative Exploration.** Guided by this global prior, the agent enters a dynamic Chain-of-Thought (CoT) reasoning loop

(Figure 2). It actively invokes a Perspective Projection tool by predicting specific spatial parameters: {azimuth, elevation, fov}.

This tool performs Equirectangular-to-Perspective (E2P) projection, rendering a distortion-free local planar view. The agent evaluates this view, articulates visual evidence in its CoT scratchpad, and updates the camera parameters. By progressively decreasing its FoV, the model executes a coarse-to-fine zooming trajectory until the object is precisely localized, culminating in the final BFoV prediction.

### 3.3 Progressive Optimization Pipeline

We optimize EAGLE-360 using a phased training pipeline, transitioning from structured format alignment to embodied trajectory maximization.

**Phase 1: Supervised Fine-Tuning (SFT).** We train the model on 20,000 multi-turn expert trajectories via next-token prediction applied strictly to action tokens. This establishes the fundamental interaction paradigm: invoking the projection tool, formatting spatial coordinates, and interleaving CoT reasoning with active observation.

**Phase 2: Group Relative Policy Optimization (GRPO).** To surpass the limitations of imitation learning and directly optimize multi-turn search behaviors, we apply GRPO in a live rollout environment. For each sample, a group  $\mathcal{G}$  of  $G$  independent trajectories is collected. The advantage for the  $i$ -th trajectory is estimated relative to the group mean, eliminating the need for a separate value network:

$$\hat{A}_i = \frac{r_i - \mu_{\mathcal{G}}}{\sigma_{\mathcal{G}} + \epsilon}, \quad (5)$$

where  $\mu_{\mathcal{G}}$  and  $\sigma_{\mathcal{G}}$  are the group mean and standard deviation,  $\epsilon$  is a stabilization constant, and  $r_i$  is a composite reward:

$$r = w_a \cdot r_{\text{ans}} + w_t \cdot r_{\text{tool}} + w_f \cdot r_{\text{fmt}} + w_l \cdot r_{\text{len}} + w_{\tau} \cdot r_{\tau}. \quad (6)$$

The reward components balance precision with exploration efficiency:

- **Answer Reward ( $r_{\text{ans}}$ ):** The primary success signal evaluating the final predicted coordinates. We designed three variations for this reward: BFoV Accuracy (a binary signal based on Eq. (2)), Mean Great Circle Distance (GCD, a continuous spatial error), and a weighted combination of both. As demonstrated in our ablation studies, utilizing the

discrete BFoV Accuracy yields the most effective optimization and best overall performance.

- **Tool-Use & Turn Efficiency ( $r_{\text{tool}}, r_{\tau}$ ):** Assigns bonuses for efficient tool usage and task completion within 1–4 turns. To penalize search exhaustion, this reward degrades to  $-0.7$  at 5 turns,  $-0.8$  at 6 turns, and  $-1.0$  beyond 6 turns or upon failure.
- **Format Correctness ( $r_{\text{fmt}} \in [0, 1]$ ):** A fractional score enforcing adherence to tool-call and XML answer tag structures.
- **Length Penalty ( $r_{\text{len}} \leq 0$ ):** A penalty on overly verbose CoT generation, discouraging the agent from artificially inflating its reasoning scratchpad to delay decisions.

The policy is updated using a PPO-style clipped surrogate objective, augmented by a KL-divergence penalty against the Phase 1 reference policy to ensure training stability and mitigate reward hacking. The complete configuration, including the formal definition of our multi-component reward function, is outlined in Appendix C.

## 4 Dataset

We introduce EAGLE-360, a comprehensive multi-turn dialogue dataset tailored for active panoramic object search. It comprises over 14,000 high-resolution panoramas (4K–8K) from diverse in-the-wild and indoor environments (Kuula (Kuula, 2026), 2D-3D-Semantics (Armeni et al., 2017), Matterport3D (Chang et al., 2017)), yielding 60,000 rendered perspective views and 70,000 reasoning turns. To address inherent dataset biases and edge continuity issues, we implement a four-direction horizontal rotation augmentation. This strategy not only effectively supplements the scarcity of "back-view" data but also guarantees a strictly uniform azimuthal distribution of target objects across all viewing angles, intrinsically enhancing the agent’s pano-coordinate modeling and rotational invariance.

### 4.1 Trajectory Synthesis and Quality Assurance

Following dense object detection via GroundingDINO (Liu et al., 2025), we utilize GPT-4o-mini (OpenAI, 2024) as a semantic filter to select referentially unique and appropriately sized targets.

Table 1: Quantitative results of open-source, proprietary, and fine-tuned models on EAGLE-360 dataset. Top-three performances are highlighted with red, green and blue.

Method	Acc.	GCD	GCD @	Fail	All Directions Acc. (%) $\uparrow$					
	(%) $\uparrow$	( $^{\circ}$ ) $\downarrow$	50 $^{\circ}$ (%) $\uparrow$	(%) $\downarrow$	Front	Back	Left	Right	Top	Bottom
<b>Proprietary Models</b>										
GPT-4o(OpenAI, 2024)	7.50	44.26	80.00	6.39	10.31	2.70	6.67	8.89	25	0
Gemini-2.5-Pro(Comanici et al., 2025)	20.28	48.89	78.61	18.33	21.65	4.05	25.56	25.56	50	20
<b>Open-source Models</b>										
Gemma-3-4b-it(Kamath et al., 2025)	1.39	95.23	25	10.83	5.15	0	0	0	0	0
Gemma-3-12b-it(Kamath et al., 2025)	2.78	88.11	30.83	12.78	4.12	0	0	6.67	0	0
InternVL3.5-4b (Wang et al., 2025)	4.72	77.7	33.06	4.17	2.06	2.70	3.33	11.11	0	0
InternVL3.5-8b (Wang et al., 2025)	5.28	82.22	30	3.89	19.59	0	0	0	0	0
Qwen2.5-VL-7B-Instruct (Bai et al., 2025b)	2.78	101.10	22.60	20.28	9.28	0	1.11	0	0	0
Qwen3-VL-4B-Instruct (Bai et al., 2025a)	8.33	54.89	57.22	6.11	15.46	1.35	4.44	11.11	0	0
Qwen3-VL-8B-Instruct (Bai et al., 2025a)	8.33	54.72	69.17	13.06	20.62	4.05	3.33	4.44	0	0
<b>Fine-tuned Models</b>										
HVS-3B (Yu et al., 2025)	11.11	41.77	77.54	7.22	18.56	10.81	7.87	7.78	0	0
EAGLE-360 (w/o FOV)	39.44	17.54	94.02	1.11	48.45	28.38	41.11	36.67	50	40
EAGLE-360 (w/o RoPE Rolling)	46.01	16.15	94.72	2.7	46.18	45.65	45.25	47.15	60	31.58
EAGLE-360 (w/o GRPO)	46.94	14.03	97.22	0.83	55.67	41.89	43.44	44.44	75	40
EAGLE-360	64.44	16.89	96.12	2.05	72.16	60.81	55.56	71.11	75	40

Crucially, we formulate the search process as a holistic *global-to-local* exploration paradigm, explicitly shifting away from myopic, iterative adjustments of localized initial views. The agent leverages spatial common sense to assess the complete 360 $^{\circ}$  context, transitioning into a localized refinement phase that progressively narrows the Field of View (FoV) to precisely bound the target. To eliminate AI hallucinations, expert annotators conducted 100 hours of rigorous inspection, enforcing absolute *Scale Validity* and *Referential Uniqueness* within the panorama.

## 4.2 Multi-turn Trajectory Formatting

To explicitly foster spatial reasoning and tool-use capabilities, each trajectory is structured as a continuous *Thought–Action–Observation* sequence. The *Thought* component serves as a Chain-of-Thought (CoT) scratchpad for articulating spatial priors. The *Action* strictly invokes an environmental tool: `rotate_and_project(az, el, fov)`. Finally, the *Observation* provides the corresponding perspective crop or a negative textual constraint if the target remains out of view. This format also preserves failed views in the dialogue history, helping the model revise its search direction in later turns. Comprehensive statistics, augmentation strategies, and the exact prompts used for data synthesis are detailed in Appendix B.

## 5 Experiment

### 5.1 Experiment Setup

**Implementation Details.** Our training pipeline consists of two stages: Supervised Fine-Tuning (SFT) and Group Relative Policy Optimization (GRPO). We utilized Qwen3-VL-4B-Instruct (Bai et al., 2025a) as our base model. During the SFT phase, we froze the Vision Encoder and the cross-modal projection layer, applying Low-Rank Adaptation (LoRA) to the Large Language Model (LLM) backbone. The model was trained on the EAGLE-360 dataset for 4 epochs to acquire the basic global-to-local tool-calling format. Subsequently, we applied GRPO to optimize the multi-turn reasoning and search trajectories, reinforcing the agent’s ability to iteratively narrow down the search space in ultra-long contexts.

**Testing Setup.** To comprehensively evaluate our method, we benchmarked EAGLE-360 against a diverse array of open-source models (e.g., Gemma-3, InternVL3.5 (Wang et al., 2025), Qwen-VL (Bai et al., 2025b,a) series), proprietary models (GPT-4o (OpenAI, 2024), Gemini-2.5-Pro (Comanici et al., 2025)), and the fine-tuned panoramic model HVS-3B (Yu et al., 2025). For existing models that rely on initial perspective priors, we evaluated them under a rigorous **random initial viewpoint** setting to ensure a fair comparison. This demonstrates EAGLE-360’s capability to autonomously com-

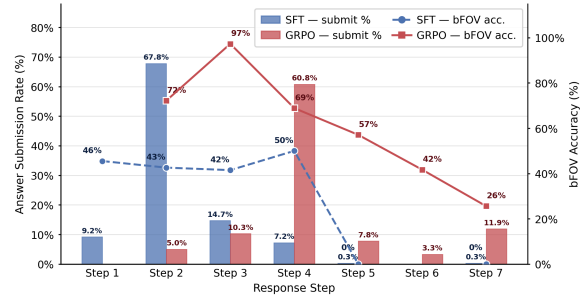
plete search tasks directly from a global 360° view without prior initialization. Furthermore, to verify zero-shot generalization, we conducted transfer evaluations on the out-of-distribution H\*Bench (Yu et al., 2025). H\*Bench comprises two core embodied tasks: Humanoid Object Search (HOS) and Humanoid Path Search (HPS).

**Evaluation Metrics.** To accurately measure localization performance in spherical spaces, we discard traditional 2D pixel-based errors and utilize a tailored metric system:

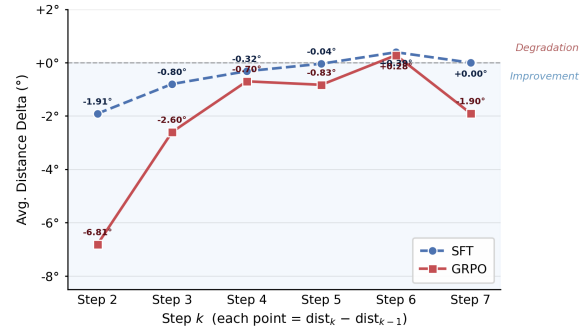
- **Mean Great Circle Distance (GCD):** Measures the shortest distance along the spherical surface between the predicted and ground truth coordinates. Lower is better.
- **GCD@50°:** The percentage of predictions where  $GCD < 50^\circ$ . This indicates successful global macroscopic perception, guaranteeing the target falls within a standard 100° FoV projection.
- **Accuracy (Acc.):** Traditional 2D bounding boxes fail at panorama boundaries and poles. We adopt an adaptive spherical threshold  $\tau = \frac{1}{2}\sqrt{w_{fov}^2 + h_{fov}^2}$ , where  $w_{fov}$  and  $h_{fov}$  are the effective FoV spans. A prediction is a “Hit” if  $GCD \leq \tau$ .
- **Fail Rate & Avg Turns:** The percentage of trajectories failing to output valid localization, and the average number of reasoning/tool-calling steps per episode.

## 5.2 Main Results

**Performance on EAGLE-360.** Table 1 presents the quantitative results on the EAGLE-360 test set. Standard open-source models process panoramas as planar images and fail catastrophically; the strongest base model, Qwen3-VL-8B-Instruct (Bai et al., 2025a), achieves only an 8.33% Accuracy. Even powerful proprietary models struggle, with GPT-4o (OpenAI, 2024) and Gemini-2.5-Pro (Comanici et al., 2025) reaching only 7.50% and 20.28%, respectively. Similarly, the prior-dependent HVS-3B (Yu et al., 2025) yields a mere 11.11% accuracy under the random initialization setting. These results suggest that panoramic search requires more than recognizing objects in local crops. The model must maintain a global spherical prior, recover from misleading views, and decide when to zoom or submit.



(a) Step-wise submission and accuracy



(b) Step-wise spatial refinement

Figure 3: Analysis of multi-turn reasoning dynamics. **(a) Step-wise submission and accuracy** illustrates that GRPO delays answer submission to promote deliberate exploration. **(b) Step-wise spatial refinement** demonstrates rapid spatial convergence in early steps, followed by diminishing returns in extended trajectories reflecting increased task uncertainty.

In stark contrast, EAGLE-360 establishes a new state-of-the-art. It boosts the overall Accuracy to a staggering 64.44%—nearly an 8-fold relative increase over the base model—and achieves a 94.72% rate for  $GCD < 50^\circ$ . Fine-grained directional analysis reveals that EAGLE-360 resolves boundary truncation issues, achieving 60.81%, 55.56% and 71.11% accuracy in the traditionally challenging “Back” “Left” and “Right” regions, validating the efficacy of our holistic perception design.

Partial results of our EAGLE-360 inference visualization pipeline are presented in Appendix D.

**Zero-Shot Transferability.** Table 2 highlights the robust generalization of our method. While EAGLE-360 is primarily aligned with the target localization objective of Humanoid Object Search (HOS), where it dominates with a score of **74.8** (vs. HVS-3B (Yu et al., 2025)’s 47.3), the Humanoid Path Search (HPS) acts as a rigorous zero-shot transfer task. Remarkably, even without explicit navigation or pathing training, EAGLE-360 achieves an HPS score of 28.0. This performance

Table 2: Transfer evaluation on H\*Bench

Method	Overall↑	HOS↑	HPS↑
GPT-4o	21.3	19.7	23.6
Gemini-2.5-Pro	32.3	31.9	<b>33</b>
InternVL3.5-4B	3.8	3.2	4.8
InternVL3.5-8B	6.7	6.4	7.2
Qwen3-VL-8B	19.1	23.6	12.2
Qwen3.5-9B	18.9	21.8	14.5
HVS-3B	38.4	47.3	24.9
EAGLE-360(w/o GRPO)	48.70	62.33	28.25
EAGLE-360	<b>56.1</b>	<b>74.8</b>	<b>28</b>

Table 3: Ablation results of GRPO with different reward on EAGLE-360.

Method	ACC(%)↑	GCD(°)↓	Fail(%)↓	Avg Turns
SFT	46.94	<b>14.03</b>	0.83	2.26
GRPO(ACC)	<b>64.44</b>	16.89	2.7	4.33
GRPO(GCD)	50.83	16.72	1.67	3.36
GRPO(ACC+GCD)	47.22	15.25	<b>0</b>	2.95

eclipses the previous SOTA HVS-3B (Yu et al., 2025) (24.9) and is highly competitive with the proprietary Gemini-2.5-Pro (Comanici et al., 2025) (33.0). This confirms that our framework learns generalized, embodied spatial reasoning rather than merely overfitting to the training distribution.

### 5.3 Ablation Studies

We conduct extensive ablation studies to isolate the contributions of our architectural and training innovations.

**Effect of Global-to-Local Framework.** A core innovation of our framework is the progressive search mechanism driven by dynamically adjustable Field of View (FoV). As shown in Table 1, removing this module (EAGLE-360 w/o FOV) causes a catastrophic drop in overall accuracy, plummeting from 64.44% to 39.44%. This highlights that standard static viewpoints are insufficient for 360-degree environments. By iteratively narrowing the FoV to zoom in, our agent effectively filters out background noise and performs fine-grained spatial verification, proving the necessity of our global-to-local paradigm.

**Effect of RoPE Rolling.** Similarly, removing the RoPE Rolling module (comparing SFT variants) degrades accuracy to 46.01%. Because standard positional encodings break the cylindrical wrap-around topology of panoramas, the model loses its rotational consistency. RoPE Rolling bridges the visual seam across the left and right boundaries at the attention level, proving indispens-

able for locating targets situated behind the camera.

**Multi-Turn Reasoning Dynamics.** Figure 3 validates the effectiveness of our Chain-of-Thought (CoT) and multi-turn tool-calling framework for panoramic search. During the SFT phase, the model tends to make premature guesses, with answer submissions peaking at Step 2 (Figure 3a). GRPO effectively shifts this distribution, pushing the submission peak to Steps 4 and 5, demonstrating that the agent learns to deliberately explore and refine its search space. Figure 3b further shows that this iterative process yields massive spatial refinement in early steps (e.g., a  $-6.81^\circ$  distance delta at Step 2). We observe that accuracy and distance improvements degrade at extended steps (Steps 6-7). This is an expected dynamic: episodes requiring excessive turns typically represent extreme edge cases (e.g., severe occlusion or ambiguous targets) where the model’s intrinsic confidence is low.

**GRPO and Reward Design.** Table 3 details the impact of our reinforcement learning alignment. Transitioning from SFT to GRPO(ACC) yields a massive performance leap (from 46.94% to **64.44%** Acc). We note an expected trade-off here: while GRPO(ACC) results in significantly more successful “Hits”, the average GCD among all samples slightly increases from  $14.03^\circ$  (SFT) to  $16.89^\circ$ , as the policy prioritizes discrete task completion over absolute continuous precision.

Furthermore, we ablated trajectory-level reward functions: ACC (discrete BFoV threshold), GCD (continuous distance), and ACC+GCD. Empirical results show that blending continuous spatial distance with discrete classification logic introduces severe gradient conflicts during policy optimization. The model becomes overly cautious, attempting to minimize GCD without confidently executing the final localization step. While this hybrid reward perfectly stabilizes the agent’s formatting (yielding a **0% Fail Rate**), it paradoxically reduces the average turns (2.95) and degrades the final accuracy (47.22%). Thus, a direct, threshold-based Accuracy reward provides the most effective supervisory signal.

## 6 Discussion and Future Work

Our EAGLE-360 framework demonstrates the potential of Multimodal Large Language Models for autonomous panoramic object localization via a global-to-local active exploration paradigm and modality-aligned RoPE Rolling. Crucially, we

overcame the computational and reward-hacking challenges inherent in ultra-long visual dialogues by leveraging Group Relative Policy Optimization (GRPO). This shift from Supervised Fine-Tuning (SFT) to GRPO empowered the policy to move beyond brittle trajectory mimicry, enabling deliberate, coarse-to-fine spatial reasoning.

Looking ahead, while our current formulation excels in static panoramic environments, real-world navigation is inherently dynamic. Our future work will focus on extending this framework into video-based and 4D spatio-temporal domains. Furthermore, as embodied agents continuously collect and process sensitive indoor panoramic data, ensuring data privacy becomes critical. Future explorations could integrate privacy-preserving decentralized training paradigms, drawing inspiration from recent advancements in class-heterogeneous federated learning for dense prediction tasks (Miao et al., 2023), to safely scale embodied agents across diverse, unconstrained physical spaces.

## Limitations

While EAGLE-360 establishes a new state-of-the-art for autonomous panoramic search, several limitations remain that warrant future investigation.

**Context Length and Inference Latency.** Our global-to-local paradigm relies on multi-turn Chain-of-Thought (CoT) reasoning combined with dynamic visual tool calling. As an episode progresses, accumulating multiple high-resolution perspective images alongside extensive textual reasoning histories results in ultra-long context windows. Due to the quadratic computational complexity of the standard Transformer attention mechanism, this massive token accumulation leads to significant memory overhead and slow autoregressive inference speeds. Consequently, deploying EAGLE-360 for high-frequency, real-time robotic navigation remains challenging without further optimizations, such as KV-cache compression or linear-complexity backbones.

**Polar Region Distortion.** Secondly, while our RoPE Rolling mechanism effectively resolves the left-right seam discontinuity, localization performance in the extreme polar regions (zenith and nadir, corresponding to the "Top" and "Bottom" directions) still slightly lags behind equatorial directions. Equirectangular projections suffer from severe, non-linear geometric warping at the poles, where pixels are dramatically stretched. During the

Stage 1 global perception phase, this extreme distortion can disrupt the vision encoder’s structural understanding, occasionally leading to sub-optimal initial viewpoint estimates before the Stage 2 local refinement can intervene. Developing distortion-aware patching strategies or fully spherical feature representations remains an important avenue for fully standardizing 360° perception.

## References

- Yuzhuo Ao, Anbang Wang, Yu-Wing Tai, and Chi-Keung Tang. 2026. [ReasonNavi: Human-inspired global map reasoning for zero-shot embodied navigation](#). *arXiv preprint arXiv:2602.15864*.
- Iro Armeni, Sasha Sax, Amir Zamir, and Silvio Savarese. 2017. [Joint 2d-3d-semantic data for indoor scene understanding](#). *ArXiv*, abs/1702.01105.
- Shuai Bai, Yuxuan Cai, Ruizhe Chen, Keqin Chen, Xionghui Chen, Zesen Cheng, Lianghao Deng, Wei Ding, Chang Gao, Chunjiang Ge, Wenbin Ge, Zhifang Guo, Qidong Huang, Jie Huang, Fei Huang, Binyuan Hui, Shutong Jiang, Zhaohai Li, Mingsheng Li, and 45 others. 2025a. Qwen3-vl technical report. *arXiv preprint arXiv:2511.21631*.
- Shuai Bai, Keqin Chen, Xuejing Liu, Jialin Wang, Wenbin Ge, Sibao Song, Kai Dang, Peng Wang, Shijie Wang, Jun Tang, Humen Zhong, Yuanzhi Zhu, Mingkun Yang, Zhaohai Li, Jianqiang Wan, Pengfei Wang, Wei Ding, Zheren Fu, Yiheng Xu, and 8 others. 2025b. Qwen2.5-vl technical report. *arXiv preprint arXiv:2502.13923*.
- Yaniv Benny and Lior Wolf. 2025. Sphereformer: A u-shaped transformer for spherical 360 perception. In *Proceedings of the IEEE/CVF Conference on Computer Vision and Pattern Recognition (CVPR)*, pages 940–950.
- Angel X. Chang, Angela Dai, Thomas A. Funkhouser, Maciej Halber, Matthias Nießner, Manolis Savva, Shuran Song, Andy Zeng, and Yinda Zhang. 2017. [Matterport3d: Learning from rgb-d data in indoor environments](#). *2017 International Conference on 3D Vision (3DV)*, pages 667–676.
- Qixiang Chen, Cheng Zhang, Chi-Wing Fu, Jing Christine Ye, and Jianfei Cai. 2025. [Openview: Empowering mllms with out-of-view vqa](#). *ArXiv*, abs/2512.18563.
- Shih-Han Chou, Wei-Lun Chao, Wei-Sheng Lai, Min Sun, and Ming-Hsuan Yang. 2020a. Visual question answering on 360deg images. In *Proceedings of the IEEE/CVF winter conference on applications of computer vision*, pages 1607–1616.
- Shih-Han Chou, Wei-Lun Chao, Wei-Sheng Lai, Min Sun, and Ming-Hsuan Yang. 2020b. Visual question answering on 360deg images. In *Proceedings of*

- the *IEEE/CVF winter conference on applications of computer vision*, pages 1607–1616.
- Shih-Han Chou, Cheng Sun, Wen-Yen Chang, Wan-Ting Hsu, Min Sun, and Jianlong Fu. 2020c. 360-indoor: Towards learning real-world objects in 360deg indoor equirectangular images. In *Proceedings of the IEEE/CVF Winter Conference on Applications of Computer Vision (WACV)*.
- Volkan Cirik, Taylor Berg-Kirkpatrick, and Louis-Philippe Morency. 2020. [Refer360°: A referring expression recognition dataset in 360° images](#). In *Proceedings of the 58th Annual Meeting of the Association for Computational Linguistics*, pages 7189–7202, Online. Association for Computational Linguistics.
- Taco S. Cohen, Mario Geiger, Jonas Köhler, and Max Welling. 2018. [Spherical cnns](#). In *International Conference on Learning Representations*.
- Gheorghe Comanici, Eric Bieber, Mike Schaekermann, Ice Pasupat, Noveen Sachdeva, Inderjit Dhillon, Marcel Blistein, Ori Ram, Dan Zhang, Evan Rosen, and 1 others. 2025. Gemini 2.5: Pushing the frontier with advanced reasoning, multimodality, long context, and next generation agentic capabilities. *arXiv preprint arXiv:2507.06261*.
- Zihao Dongfang, Xu Zheng, Ziqiao Weng, Yuanhuiyi Lyu, Danda Pani Paudel, Luc van Gool, Kailun Yang, and Xuming Hu. 2025. [Are multimodal large language models ready for omnidirectional spatial reasoning?](#) *ArXiv*, abs/2505.11907.
- Edward J Hu, Yelong Shen, Phillip Wallis, Zeyuan Allen-Zhu, Yuanzhi Li, Shean Wang, Liang Wang, Weizhu Chen, and 1 others. 2022. Lora: Low-rank adaptation of large language models. *Iclr*, 1(2):3.
- Gemma Team Aishwarya Kamath, Johan Ferret, Shreya Pathak, Nino Vieillard, Ramona Merhej, Sarah Perrin, Tatiana Matejovicova, Alexandre Ramé, Morgane Rivière, Louis Rouillard, Thomas Mesnard, Geoffrey Cideron, Jean-Bastien Grill, Sabela Ramos, Edouard Yvinec, Michelle Casbon, Etienne Pot, Ivo Penchev, Gael Liu, and 191 others. 2025. [Gemma 3 technical report](#). *ArXiv*, abs/2503.19786.
- Mukul Khanna, Ram Ramrakhya, Gunjan Chhablani, Sriram Yenamandra, Theophile Gervet, Matthew Chang, Zsolt Kira, Devendra Singh Chaplot, Dhruv Batra, and Roozbeh Mottaghi. 2024. Goat-bench: A benchmark for multi-modal lifelong navigation. In *Proceedings of the IEEE/CVF Conference on Computer Vision and Pattern Recognition*, pages 16373–16383.
- Kuula. 2026. Kuula: 360 virtual tours and panoramic images. <https://kuula.co/>. Accessed: 2026-05.
- Woosuk Kwon, Zhuohan Li, Siyuan Zhuang, Ying Sheng, Lianmin Zheng, Cody Hao Yu, Joseph Gonzalez, Hao Zhang, and Ion Stoica. 2023. [Efficient memory management for large language model serving with pagedattention](#). In *Proceedings of the 29th Symposium on Operating Systems Principles, SOSP '23*, page 611–626, New York, NY, USA. Association for Computing Machinery.
- Ze Lin and Xu Zheng. 2026. [Panoenv: Exploring 3d spatial intelligence in panoramic environments with reinforcement learning](#). *ArXiv*, abs/2602.21992.
- Zhixin Ling, Zhen Xing, Xiangdong Zhou, Manliang Cao, and Guichun Zhou. 2023. Panoswin: A panostyle swin transformer for panorama understanding. In *Proceedings of the IEEE/CVF Conference on Computer Vision and Pattern Recognition (CVPR)*, pages 17755–17764.
- Shilong Liu, Zhaoyang Zeng, Tianhe Ren, Feng Li, Hao Zhang, Jie Yang, Qing Jiang, Chunyuan Li, Jianwei Yang, Hang Su, Jun Zhu, and Lei Zhang. 2025. Grounding dino: Marrying dino with grounded pre-training for open-set object detection. In *Computer Vision – ECCV 2024*, pages 38–55, Cham. Springer Nature Switzerland.
- Jiaxu Miao, Zongxin Yang, Leilei Fan, and Yi Yang. 2023. [Fedseg: Class-heterogeneous federated learning for semantic segmentation](#). In *2023 IEEE/CVF Conference on Computer Vision and Pattern Recognition (CVPR)*, pages 8042–8052.
- OpenAI. 2024. [Hello gpt-4o](#).
- Yuankai Qi, Qi Wu, Peter Anderson, Xin Wang, William Yang Wang, Chunhua Shen, and Anton van den Hengel. 2020. Reverie: Remote embodied visual referring expression in real indoor environments. In *Proceedings of the IEEE/CVF Conference on Computer Vision and Pattern Recognition (CVPR)*.
- Ram Ramrakhya, Eric Undersander, Dhruv Batra, and Abhishek Das. 2022. Habitat-web: Learning embodied object-search strategies from human demonstrations at scale. In *Proceedings of the IEEE/CVF Conference on Computer Vision and Pattern Recognition (CVPR)*, pages 5173–5183.
- Jeff Rasley, Samyam Rajbhandari, Olatunji Ruwase, and Yuxiong He. 2020. [Deepspeed: System optimizations enable training deep learning models with over 100 billion parameters](#). In *Proceedings of the 26th ACM SIGKDD International Conference on Knowledge Discovery & Data Mining, KDD '20*, page 3505–3506, New York, NY, USA. Association for Computing Machinery.
- Jiahui Ren, Mochu Xiang, Jiajun Zhu, and Yuchao Dai. 2025. Panosplatt3r: Leveraging perspective pretraining for generalized unposed wide-baseline panorama reconstruction. In *Proceedings of the IEEE/CVF International Conference on Computer Vision (ICCV)*, pages 28959–28969.
- Zhihong Shao, Peiyi Wang, Qihao Zhu, Runxin Xu, Jun-Mei Song, Mingchuan Zhang, Y. K. Li, Yu Wu, and Daya Guo. 2024. [Deepseekmath: Pushing the limits](#)

- of mathematical reasoning in open language models. *ArXiv*, abs/2402.03300.
- Guangming Sheng, Chi Zhang, Zilingfeng Ye, Xibin Wu, Wang Zhang, Ru Zhang, Yanghua Peng, Haibin Lin, and Chuan Wu. 2024. Hybridflow: A flexible and efficient rlhf framework. *arXiv preprint arXiv:2409.19256*.
- Cheng Sun, Chi-Wei Hsiao, Min Sun, and Hwann-Tzong Chen. 2019. [HorizonNet: Learning room layout with 1d representation and pano stretch data augmentation](#). In *Proceedings of the IEEE/CVF Conference on Computer Vision and Pattern Recognition*, pages 1047–1056.
- Cheng Sun, Min Sun, and Hwann-Tzong Chen. 2021. [HoHoNet: 360 indoor holistic understanding with latent horizontal features](#). In *Proceedings of the IEEE/CVF Conference on Computer Vision and Pattern Recognition*, pages 2573–2582.
- Huyen-Tran Tran, Van-Quang Nguyen, Farros Alferro, Kanglin Liu, and Takayuki Okatani. 2026. [360° image perception with mllms: A comprehensive benchmark and a training-free method](#).
- Weiyun Wang, Zhangwei Gao, Lixin Gu, Hengjun Pu, Long Cui, Xingguang Wei, Zhaoyang Liu, Linglin Jing, Shenglong Ye, Jie Shao, and 1 others. 2025. Internvl3. 5: Advancing open-source multimodal models in versatility, reasoning, and efficiency. *arXiv preprint arXiv:2508.18265*.
- Liu Yang, Huiyu Duan, Ran Tao, Juntao Cheng, Sijing Wu, Yunhao Li, Jing Liu, Xiongkuo Min, and Guangtao Zhai. 2025. [Odi-bench: Can mllms understand immersive omnidirectional environments?](#) *ArXiv*, abs/2510.11549.
- Naoki Yokoyama, Ram Ramrakhya, Abhishek Das, Dhruv Batra, and Sehoon Ha. 2024. [Hm3d-ovon: A dataset and benchmark for open-vocabulary object goal navigation](#). In *2024 IEEE/RSJ International Conference on Intelligent Robots and Systems (IROS)*, pages 5543–5550. IEEE.
- Heyang Yu, Yinan Han, Xiangyu Zhang, Baiqiao Yin, Bowen Chang, Xiangyu Han, Xinhao Liu, Jing Zhang, Marco Pavone, Chen Feng, Saining Xie, and Yiming Li. 2025. [Thinking in 360°: Humanoid visual search in the wild](#). *arXiv preprint arXiv:2511.20351*.
- Heeseung Yun, Youngjae Yu, Wonsuk Yang, Kangil Lee, and Gunhee Kim. 2021. [Pano-avqa: Grounded audio-visual question answering on 360° videos](#). In *Proceedings of the IEEE/CVF International Conference on Computer Vision*, pages 2031–2041.
- Jiazhao Zhang, Kunyu Wang, Rongtao Xu, Gengze Zhou, Yicong Hong, Xiaomeng Fang, Qi Wu, Zhizheng Zhang, and Wangui He. 2024. [Navid: Video-based vlm plans the next step for vision-and-language navigation](#). *ArXiv*, abs/2402.15852.
- Wenqi Zhang, Mengna Wang, Gangao Liu, Huixin Xu, Yiwei Jiang, Yongliang Shen, Guiyang Hou, Zhe Zheng, Hang Zhang, Xin Li, Weiming Lu, Peng Li, and Yueting Zhuang. 2025a. [Embodied-reasoner: Synergizing visual search, reasoning, and action for embodied interactive tasks](#). *arXiv preprint arXiv:2503.21696*.
- Xinshen Zhang, Zhen Ye, and Xu Zheng. 2025b. [Towards omnidirectional reasoning with 360-r1: A dataset, benchmark, and grpo-based method](#). *arXiv preprint arXiv:2505.14197*.
- Duo Zheng, Shijia Huang, Lin Zhao, Yiwu Zhong, and Liwei Wang. 2024. [Towards learning a generalist model for embodied navigation](#). In *Proceedings of the IEEE/CVF Conference on Computer Vision and Pattern Recognition (CVPR)*, pages 13624–13634.
- Gengze Zhou, Yicong Hong, and Qi Wu. 2024. [Navgpt: Explicit reasoning in vision-and-language navigation with large language models](#). *Proceedings of the AAAI Conference on Artificial Intelligence*, 38(7):7641–7649.
- Yikang Zhou, Tao Zhang, Dizhe Zhang, Shunping Ji, Xiangtai Li, and Lu Qi. 2025. [Dense360: Dense understanding from omnidirectional panoramas](#). *ArXiv*, abs/2506.14471.
- Muzhi Zhu, Hao Zhong, Canyu Zhao, Zongze Du, Zheng Huang, Mingyu Liu, Hao Chen, Cheng Zou, Jingdong Chen, Ming Yang, and Chunhua Shen. 2025. [Active-o3: Empowering multimodal large language models with active perception via grpo](#). *ArXiv*, abs/2505.21457.

## A Code and Reproducibility

To facilitate reproducibility and strictly adhere to the double-blind review process, we have anonymized and open-sourced the complete implementation of **EAGLE-360**. The repository includes the core code for the RoPE Rolling mechanism, the multi-turn active exploration environment wrapper, the tool-augmented baseline configurations, and the full multi-phase training pipeline scripts (SFT and GRPO). The source code is publicly accessible at the following repository: <https://github.com/Sansju/EAGLE-360>

## B Dataset Details

### B.1 EAGLE-360 Dataset Composition

Table 4 summarizes the panorama sources for the EAGLE-360 dataset. Our corpus contains a meticulously filtered subset of 3,609 high-quality original panoramas, which is expanded to 14,436 through data augmentation, collected from a diverse mix of academic datasets and public internet platforms. The panoramic imagery spans a wide range of resolutions, from  $2048 \times 1024$  to  $8192 \times 4096$ , with the vast majority of the data concentrated at the high-fidelity  $4096 \times 2048$  resolution. This high pixel density is crucial for preserving fine-grained visual details and minimizing distortion artifacts during the spherical-to-planar projection process.

The dataset is strategically composed to encompass diverse environmental topologies. It incorporates complex residential and commercial indoor spaces from Matterport3D (Chang et al., 2017), alongside structured academic and office environments from 2D-3D-Semantics (Armeni et al., 2017). These indoor scenes provide object-rich local layouts, varying depth relations, and dense semantic contexts essential for indoor spatial reasoning. To complement this, we integrate in-the-wild panoramas from Kuula (Kuula, 2026), which introduce outdoor landscapes, aerial views, and mixed-type scenes. This balance is important for pano-native spatial learning, ensuring the model generalizes across both constrained indoor spatial layouts and expansive outdoor environments with long-range visibility.

Given our use of large-scale panoramic imagery, we carefully address licensing, privacy, and potential misuse considerations. The EAGLE-360 corpus strictly utilizes existing panoramic datasets and publicly accessible web sources. We properly cite all external datasets and model components used in

this work, and will release only the assets whose redistribution is fully compatible with the corresponding source licenses, data-use agreements, and terms of service. Because panoramic imagery captures  $360^\circ$  continuous views, it inherently carries a risk of inadvertently containing homes, bystanders, vehicles, or other sensitive visual details. Prior to the public release, we apply rigorous privacy-oriented filtering to remove or mask personally identifying content where applicable, exclude unsafe or sensitive scenes, and establish a dedicated removal channel for reporting problematic examples.

Table 4: Statistical Breakdown and Scene Types of Data Sources

Data Source	Original Images	Filtered Images	Augmented Images	Projected Images
Matterport3D	9684	3030	12120	49881
2D-3D-S	1413	449	1796	7387
Kuula	664	130	520	2155
<b>Total</b>	<b>11761</b>	<b>3609</b>	<b>14436</b>	<b>59,423</b>

### B.2 Metadata and Training Data Pipeline

We describe the full pipeline for constructing the spatial-localization training set from raw ERP panoramas. The pipeline proceeds in six stages: automated object candidate generation, geometry-grounded quality filtering, expert human curation, train/test splitting, rotation-based data augmentation, and two-stage multi-turn dialogue construction.

#### Stage 1: Automated Object Candidate Generation.

For each ERP panorama, we first render six perspective views corresponding to the standard cubemap faces (front, back, left, right, top, bottom) at a  $90^\circ$  field of view with a face resolution of  $1024 \times 1024$  pixels. Two complementary strategies are employed depending on the dataset: (i) For datasets with rich semantic structure (*i.e.*, Matterport3D (Chang et al., 2017) and 2D-3D-Semantics (Armeni et al., 2017)), we run GroundingDINO (Liu et al., 2025) with a SwinTOGC backbone (box confidence threshold 0.3, text threshold 0.25) on each cubemap face to enumerate candidate object bounding boxes. (ii) For web-sourced panoramas (*i.e.*, Kuula (Kuula, 2026)), we use GPT-4o-mini (OpenAI, 2024) (accessed via the OpenRouter API) to list all clearly identifiable objects visible in each face image. In a subsequent filtering step, GPT-4o-mini (OpenAI,

2024) is prompted to select exactly four spatially discriminative objects per panorama, subject to two hard constraints: *spatial uniqueness* (each selected object must appear in exactly one cubemap face; semantically equivalent instances across different faces are treated as duplicates) and *content specificity* (generic structural elements such as floor, wall, ceiling, or sky are excluded). For each selected object, GPT-4o-mini (OpenAI, 2024) further generates a concise, discriminative natural-language description from the annotated face image, and performs a second uniqueness check on the *full panorama* to confirm that the described object instance appears only once in the 360° scene.

### Stage 2: Geometry-Grounded Quality Filtering.

Given a candidate (panorama, object description, approximate direction) triple, we verify geometric annotation quality using GroundingDINO as a re-detection oracle. Specifically, we rotate the ERP image to center the camera on the estimated ground-truth azimuth and elevation, crop a perspective view with FoV = 100° at 1024 × 1024 pixels, and run GroundingDINO using the object’s natural-language description as the text prompt. A detection is accepted only if all three conditions are met: (a) the highest-confidence detection scores above 0.5; (b) the great-circle angular error between the detection center and the nominal ground-truth direction is less than 5°; (c) the detected bounding box does not touch any edge of the cropped image (a minimum margin of 10 pixels is required on all sides, ensuring the object is fully contained in the projection). For passing samples, we replace the original approximate ground-truth coordinates with the GroundingDINO-predicted box center, and compute the corresponding spherical bounding field of view (BFoV) by densely sampling the bounding-box perimeter and back-projecting to equirectangular coordinates.

**Stage 3: Expert Human Curation.** After automatic filtering, two domain experts independently reviewed every remaining sample and applied the following manual quality criteria:

- **Global uniqueness.** The target object must be the only instance of its kind present anywhere in the full panorama, making its azimuth–elevation position unambiguous and non-confusable.
- **Visual clarity.** The object must be clearly visible and not substantially occluded, ensur-

ing that a human or model inspecting the projected view can reliably identify and localize it.

- **Language discriminability.** The object must be describable with a concise natural-language phrase that unambiguously distinguishes it from other objects in the same scene.
- **Angular size constraints.** Objects whose BFoV spans a large fraction of the standard field of view are excluded, as they would make the localization task trivially easy. Conversely, objects whose BFoV diagonal subtends fewer than  $\sim 5^\circ$  are also excluded, as such targets are too small to be reliably found through active perspective-view exploration.

Samples passing both reviewers’ judgements were retained. Out of 11,761 raw panoramas, this stage produced 3,609 high-quality object-localization question–answer pairs spanning 2,858 unique panoramas (a total retention rate of  $\approx 31\%$ ).

**Stage 4: Train/Test Split.** The curated pairs were partitioned into a training set of 3,249 samples and a test set of 360 samples, with no panorama appearing in both splits. The source distribution is approximately preserved: Matterport3D (Chang et al., 2017) contributes 84%, 2D-3D-Semantics (Armeni et al., 2017) contributes 12.4%, and Kuula (Kuula, 2026) contributes 3.6% in both subsets.

### Stage 5: Rotation-Based Data Augmentation.

To enlarge the training set and improve rotational invariance, we apply three horizontal rotations—+90°, +180°, and +270°—to every training panorama. Each rotation is implemented as a pixel-level horizontal roll of the ERP image by a fraction  $\{1/4, 1/2, 3/4\}$  of the image width, which corresponds exactly to a rigid horizontal rotation in spherical geometry. For each augmented entry, the ground-truth azimuth is updated as  $\phi_{\text{new}} = \text{wrap}(\phi + \Delta)$  where  $\text{wrap}(\cdot)$  maps the result to  $(-\pi, \pi]$ ; the elevation, BFoV dimensions, and pixel bounding box remain unchanged. The GPT response text in the conversation is updated to reflect the new azimuth value. This augmentation produces a  $\times 4$  expansion of the training set (3,249 original  $\rightarrow$  12,996 samples), with 53,451 associated perspective-view projections stored on disk. The test set is *not* augmented.

**Stage 6: Two-Stage Multi-Turn Dialogue Construction.** For each training sample, we programmatically synthesize a multi-turn tool-call conversation that simulates an active-search agent progressively localizing the target object. The dialogue is constructed in two stages, with a maximum of  $\text{MAX\_TURN} = 6$  assistant turns.

**Coarse estimation** (up to three attempts). The first tool call is generated from a simulated coarse estimate. With probability 0.8 the estimate places the ground-truth object center within the initial  $100^\circ$  field of view (*in-FoV* case); with probability 0.2 the object is outside the field of view (*out-of-FoV* case), prompting the model to continue searching. Specifically, we compute the bounding-box visibility ratio—the fraction of the ground-truth BFoV that falls within the current perspective projection—and branch on three conditions: (i) if  $\text{visibility} \geq 1.0$ , the object is fully visible and the dialogue enters the fine-estimation stage immediately; (ii) if  $0.7 \leq \text{visibility} < 1.0$ , the object is partially visible and the next tool call moves the camera directly toward the ground-truth center; (iii) if  $\text{visibility} < 0.7$ , the object is not visible and the next estimate is drawn uniformly at random, with the probability of an in-FoV next estimate increasing across attempts (first miss:  $1/3$  in-FoV; second miss:  $2/3$  in-FoV).

**Fine estimation** (two to three rounds). Once the object is fully in view, the camera progressively zooms in using an ease-out trajectory: at each fine step, the field of view narrows linearly from  $100^\circ$  toward a target FoV computed as  $\text{FoV}_{\text{target}} = 1.2 \times \max(\text{BFoV}_{\text{az}}, \text{BFoV}_{\text{el}})$ , clamped to  $[20^\circ, 100^\circ]$ , where  $\text{BFoV}_{\text{az}}$  and  $\text{BFoV}_{\text{el}}$  are the angular extents of the ground-truth bounding field of view. With probability 0.05, a *correction scenario* is injected: the model overshoots the target (simulated by an off-center tool call that places the object outside the narrower FoV), and the subsequent turn must backtrack and reacquire the object. At the final turn, the model outputs the ground-truth azimuth and elevation as the predicted spherical coordinates.

Each tool call invokes `rotate_and_project_panorama` with azimuth, elevation, and FoV as arguments, and returns a  $512 \times 512$  perspective projection rendered on the fly. The resulting dataset contains an average of 4.11 projected images per QA pair ( $\sigma = 0.6$ ), amounting to 53,451 training images in total.

### B.3 Data Distribution

To address this, we apply a horizontal  $90^\circ$  rotation data augmentation to each view. For the horizontal direction, this process not only supplements the rear perspective but also ensures an identical data distribution across all horizontal views (front, rear, left, and right). For the polar regions, although the augmentation increases the amount of polar data, such instances remain extremely rare because target objects seldom appear in these areas. Consequently, polar data accounts for only 3.04% of our overall dataset.

### B.4 Prompt Templates

#### System Prompt

You are a helpful assistant for panoramic image understanding.

#### # Tools

You may call one or more functions to assist with the user query. You are provided with function signatures within `<tools>` XML tags:

```
<tools>
[
{
  "type": "function",
  "function": {
    "name": "rotate_and_project_panorama",
    "description": "Rotate the panoramic image to center on a specific direction and project it to a perspective view with given field of view. You need to repeatedly call it. By adjusting the azimuth and elevation angles, as well as reducing the field of view, you should gradually move the center of the viewing angle closer to the target object until a precise positioning is achieved.",
    "parameters": {
      "properties": {
        "azimuth": {
          "type": "number",
          "description": "The azimuth angle in degrees, range [-180, 180]. 0 is forward, positive is right."
        },
        "elevation": {
          "type": "number",
```

```

"description": "The elevation angle
in degrees, range [-90, 90]. 0 is
horizontal, positive is up."
},
"fov_degrees": {
"type": "number",
"description": "The field of view in
degrees. Default is 100."
}
},
"required": ["azimuth", "elevation"],
"type": "object"
},
"args_format": "Format the arguments
as a JSON object."
}
}
]

```

For the function call, return a json object with function name and arguments within `<tool_call>` `</tool_call>` XML tags:

```

<tool_call>
{"name":           <function-name>,
"arguments": <args-json-object>}
</tool_call>

```

### # Important: Tool Calling Rules

1. If you decide to call a tool, output ONLY the tool call and STOP immediately.
2. DO NOT provide the final answer in the same response as the tool call.
3. The tool will return a projected image, and you should wait for it before giving your answer.
4. Note that when calling the tool, the parameters should not be the same as those used previously.

### # Response Format

- If you can answer directly without tools: `<think>...</think>`  
`<answer>...</answer>`
- If you need to use a tool:  
`<think>...</think>`  
`<tool_call>...</tool_call>`  
(STOP HERE, wait for tool result)

- After receiving the tool result and ready to answer: `<think>...</think>`  
`<answer>...</answer>`

You MUST provide an answer within the prescribed MAX\_TURN of conversations! The MAX\_TURN of conversations is 6. NEVER combine `<tool_call>` and `<answer>` in the same response unless you have already received the projected image!

### Prompt A1: Single-face Object Enumeration (Called per cubemap face)

Analyze the image from the {direction} direction. Your task is to list the main, clearly identifiable objects.

Your descriptions should be concise and objective. Only include what is visually present in the image.

Follow these rules strictly:

1. Do not use numbers to describe the quantity of objects; use the plural form directly. For example, describe 'two chairs' simply as 'chairs'.
2. Don't describe items using horizontal directional words such as "left" or "right".
3. Ensure the correctness of the object description and try to describe objects that you are 100% certain about. If an object is difficult to identify or cannot be described in words, do not describe it.

Return your answer as a single Python list of strings.

For example:

```
["a wooden dining table", "a hanging pendant light", "a large window with sheer curtains"]
```

### Prompt A2: Select 4 Spatially Unique Objects from Six-face List

You will be given a dictionary where keys are six directions (front, back, left, right, top, bottom) and values are objects in each view.

Your task is to identify and return exactly **FOUR** best distinct objects from these descrip-

tions.

Follow these rules strictly:

1. **Unique Location:** Select only items that appear in ONE direction. You must perform a semantic check; for example, if a 'wooden chair' is in the 'left' view and a 'chair' is in the 'front' view, you cannot select it because the concept of a 'chair' exists in multiple views.
2. **Unique Items:** Do not select generic background elements. Avoid items like 'sky', 'clouds', 'ground', 'floor', 'walls', 'ceiling', or 'water'. Focus on specific, identifiable objects that are salient to the scene.

Return your answer as a Python Dictionary in *standard JSON format*.

Example Input:

```
{
  "front": ["a stone kitchen island",
  ...],
  ...
}
```

Example Output:

```
{
  "front": ["a built-in microwave",
  "a sink with a black faucet"],
  "left": ["a wall-mounted
  touchscreen control panel"],
  "right": ["a boat steering wheel"]
}
```

Input:

```
{obj_location_dict}
```

Output:

- If incorrect: "incorrect: [actual object name]"

For example:

"correct"

"incorrect: sofa"

"incorrect: dining table"

Answer:

### Prompt B2: Panorama-level Uniqueness Verification

This is a 360-degree panoramic image. Look carefully at the entire image.

Does the object "{object\_description}" appear exactly ONCE in this panoramic image, or does it appear multiple times?

Answer with only "once" or "multiple".

### Prompt B3: Detailed Object Description Generation with Bbox

Look at this image with a red bounding box. Provide a brief description with 1-2 key visual features of the object inside the box.

Keep it SHORT and simple. Examples:

- "a red leather armchair"
- "a white ceramic vase"
- "a wooden dining table"

Format: Return ONLY the description of the object in the red box, starting with "a" or "an". Maximum 10-11 words.

Description:

### Prompt B1: Bounding Box Object Label Verification and Correction

Look at this image with a red bounding box. The object detection model predicted the object inside the red box is a "{predicted\_label}".

Question 1: Is this prediction correct for the object INSIDE the red box?

Question 2: If not correct, what is the actual object inside the red box?

Please answer **STRICTLY** in this format:

- If correct: "correct"

## C Training Details

### C.1 Training Implementation Details

**Base Model.** All experiments use Qwen3-VL-4B-Instruct (Bai et al., 2025a) as the backbone. We add a single special token  $\langle | \text{panoramic\_image\_pad} | \rangle$  to the vocabulary to distinguish the panoramic modality from ordinary perspective images. Its input and output embeddings are initialised using a *noisy-mean* strategy: the new vector is set to the mean of the existing vocabulary embeddings (computed over the original 151,669 tokens) plus Gaussian noise  $\mathcal{N}(0, d^{-1/2})$ ,

where  $d$  is the embedding dimension. This strategy accelerates convergence relative to random initialization. We also patch the Qwen3-VL chat template so that `<think>` content is preserved in historical assistant turns during training; the original template strips thinking tokens from context, which would prevent the model from learning the correct chain-of-thought format.

**Stage 1: Supervised Fine-Tuning (SFT).** We fine-tune Qwen3-VL-4B-Instruct on the 12,996-sample training set using parameter-efficient LoRA (Hu et al., 2022) with the following configuration:

- **LoRA hyperparameters.** Rank  $r = 32$ , scaling  $\alpha = 32$ , dropout  $p = 0.05$ . LoRA adapters are applied to *all* linear projection layers (i.e., all `nn.Linear` modules) in both the language model and the vision-language projector, excluding `embed_tokens` and `lm_head`. The latter two modules are trained *in full* via PEFT `modules_to_save` to accommodate the new special token. The visual encoder is entirely frozen.
- **Optimisation.** AdamW, learning rate  $1 \times 10^{-5}$ , cosine decay schedule with a linear warm-up over 3% of total steps, gradient clipping at  $\ell_\infty = 1.0$ , weight decay = 0.
- **Batch and sequence.** Per-device batch size 1 with gradient accumulation over 8 steps across 2 NVIDIA RTX 6000 GPUs. Maximum sequence length 16,384 tokens. Input image resolution is bounded by `[min_pixels = 262,144, max_pixels = 2,072,312]` pixels; panoramic images are processed at the original ERP resolution within this range.
- **Mixed precision and efficiency.** BFloat16, FlashAttention-2, gradient checkpointing, and ZeRO Stage-2 offloading via DeepSpeed (Rasley et al., 2020).
- **Schedule.** 2 epochs over the full training set, taking approximately 8 hours. Checkpoints are saved every 3,000 steps.

The SFT objective is standard next-token prediction with cross-entropy loss over all assistant tokens, including both the `<think>` reasoning chain and the final `<tool_call>` or `<answer>` tokens.

## Stage 2: Reinforcement Learning via GRPO.

Starting from the SFT checkpoint, we apply Group Relative Policy Optimisation (GRPO) (Shao et al., 2024) implemented within the VERL framework (Sheng et al., 2024). This stage is executed across 4 NVIDIA RTX 6000 GPUs, requiring approximately 40 hours of training. We use a custom PanoramicRolloutManager that interleaves model generation with on-the-fly tool execution.

**Rollout.** For each training prompt the rollout manager samples  $G = 4$  independent trajectories (group size) using vLLM (Kwon et al., 2023) in synchronous mode with temperature  $\tau = 0.7$  and top- $p = 0.95$ . Each trajectory is a multi-turn dialogue capped at  $T_{\max} = 7$  turns; at every assistant turn the model either invokes the `rotate_and_project_panorama` tool (which returns a  $512 \times 512$  perspective crop at the specified azimuth, elevation, and  $100^\circ$  FoV) or emits a final `<answer>`. The maximum number of tool calls per trajectory is 8.

**Reward function.** The scalar reward  $r$  is a weighted sum of four components:

$$r = w_a \cdot r_{\text{ans}} + w_t \cdot r_{\text{tool}} + w_f \cdot r_{\text{fmt}} + w_l \cdot r_{\text{len}} \quad (7)$$

with weights  $w_a = 0.5$ ,  $w_t = 0.1$ ,  $w_f = 0.15$ ,  $w_l = 0.05$ . An additional turn-efficiency term with weight  $w_\tau = 0.2$  is added as described below.

- **Answer reward  $r_{\text{ans}}$ .** Let  $d$  denote the great-circle distance (in degrees) between the predicted and ground-truth spherical coordinates extracted from the final `<answer>` block. The reward follows a piecewise linear curve:

$$r_{\text{ans}} = \begin{cases} 1.0 & d \leq 10^\circ \\ 1.0 - 0.2 \frac{d-10}{20} & 10^\circ < d \leq 30^\circ \\ 0.8 - 0.3 \frac{d-30}{20} & 30^\circ < d \leq 50^\circ \\ 0.5 - 0.5 \frac{d-50}{40} & 50^\circ < d \leq 90^\circ \\ -0.2 & d > 90^\circ \\ -0.3 & \text{no valid } \langle \text{answer} \rangle \end{cases} \quad (8)$$

- **Tool-use reward  $r_{\text{tool}}$ .** A base bonus of +0.3 is awarded whenever at least one tool call is issued. Additional bonuses of up to +0.4 are given if the last tool call’s viewing direction is closer to the ground truth than the first, and up to +0.3 if the final answer is more accurate than the last tool call. A bonus

of +0.1 is given for using 1–3 tool calls (efficient search); using more than 5 incurs a  $-0.1$  penalty. Repeated tool calls (angular difference  $< 3^\circ$  in both azimuth and elevation and FoV difference  $< 3^\circ$ ) each incur a  $-0.15$  penalty to discourage stagnation.

- **Format reward**  $r_{\text{fmt}}$ . Each assistant turn is checked for structural compliance: non-final turns must contain valid `<think>+<tool_call>` blocks (inner content  $> 5$  characters each), and the final turn must contain valid `<think>+<answer>` blocks.  $r_{\text{fmt}} = \text{correct\_turns}/\text{total\_turns} \in [0, 1]$ .
- **Turn-efficiency reward**  $r_\tau$  (**weight**  $w_\tau = 0.2$ ). Dialogues completing in 1–4 tool calls receive a full bonus of 1.0; longer dialogues receive a linear penalty. Failing to emit any answer within the turn budget incurs a  $-1.0$  penalty.
- **Length penalty**  $r_{\text{len}}$ . A penalty of  $-0.2$  per 100 estimated tokens beyond a 256-token threshold is applied to the total assistant response length to discourage verbose outputs.

KL divergence is disabled (neither KL loss nor KL reward penalty), so the policy is updated purely via the GRPO clipped surrogate objective on normalised within-group advantages. A loss mask and a GAE mask are applied to restrict gradient computation to the assistant tokens in the most recent  $W = 2$  turns of each trajectory (sliding window), reducing memory consumption while maintaining training signal on the most informative recent context.

**Optimisation.** AdamW with learning rate  $1 \times 10^{-6}$ , cosine decay, 25-step linear warm-up (min LR ratio 0.02), and gradient checkpointing. Full-model training (no LoRA) under FSDP2 strategy on a single node. Total training: 1,000 steps, checkpoint every 250 steps, evaluation every 20 steps.

## D Case Study

In this section, we provide qualitative case studies comprising both dataset examples and inference results from EAGLE-360. First, we illustrate the rich, multi-turn nature of the conversational data constructed in our dataset. Second, we demonstrate the efficiency and precision of the EAGLE-360

framework in exploring panoramic environments and successfully localizing target objects.

### D.1 Dataset Case

See Figs. 4–6

### D.2 Inference Case

See Figs. 7–9

### 360° Panoramic Input Image



**Q:** This is a 360-degree panoramic image. Locate a pink round stool and specify its angular coordinates in degrees.

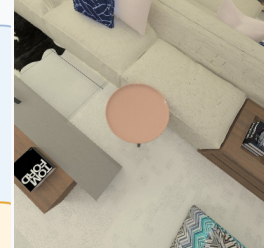
#### 1 Turn 1

##### Thinking:

Looking at this 360-degree panoramic image, I need to find a pink round stool. Analyzing the scene layout and context, I believe the object could be located around azimuth 141° and elevation -80°. I'll rotate to that direction to check.

**Tool call:** `rotate_and_project_panorama(azimuth=141.4°, elevation=-80.0°, fov_degrees=100.0°)`

Projected view (az=141.4°, el=-80.0°, fov=100.0°)



#### 2 Turn 2

##### Thinking:

The target a pink round stool is now visible positioned centrally. I should focus on that region and zoom in for a clearer observation. This will allow me to see the object in greater detail. Adjusting view to azimuth 138.6° and elevation -76.1° with FOV 65.6°.

**Tool call:** `rotate_and_project_panorama(azimuth=138.6°, elevation=-76.1°, fov_degrees=65.6°)`

Projected view (az=138.6°, el=-76.1°, fov=65.6°)



#### 3 Turn 3

##### Thinking:

The target a pink round stool is now visible in the central region. I should focus on that region and zoom in for a clearer observation. This will allow me to see the object in greater detail. Adjusting view to azimuth 137.7° and elevation -74.8° with FOV 31.2°.

**Tool call:** `rotate_and_project_panorama(azimuth=137.7°, elevation=-74.8°, fov_degrees=31.2°)`

Projected view (az=137.7°, el=-74.8°, fov=31.2°)



**Answer:** The a pink round stool is located at: - Azimuth: 137.7° - Elevation: -74.8°

Figure 4: A training data sample from kuula (Kuula, 2026)

### 360° Panoramic Input Image



**Q:** This is a 360-degree panoramic image. Could you find a bed with decorative pillows and a light blanket and provide its spherical coordinates in degrees?

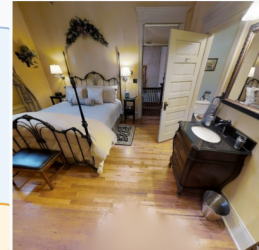
#### 1 Turn 1

##### Thinking:

The panoramic image shows a complete 360-degree view of the environment. To find a bed with decorative pillows and a light blanket, I need to analyze the scene. Considering the typical placement and visual context, I believe it could be around azimuth  $-168^\circ$  and elevation  $-29^\circ$ . I'll rotate to check.

**Tool call:** `rotate_and_project_panorama(azimuth=-168.4°, elevation=-28.7°, fov_degrees=100.0°)`

Projected view (az=-168.4°, el=-28.7°, fov=100.0°)



#### 2 Turn 2

##### Thinking:

I've spotted a bed with decorative pillows and a light blanket at the in the center-left area, but it extends beyond the edge of my current view. To see it fully, I'll rotate towards it. Moving to azimuth  $157.7^\circ$  and elevation  $-24.2^\circ$ .

**Tool call:** `rotate_and_project_panorama(azimuth=157.7°, elevation=-24.2°, fov_degrees=100.0°)`

Projected view (az=157.7°, el=-24.2°, fov=100.0°)



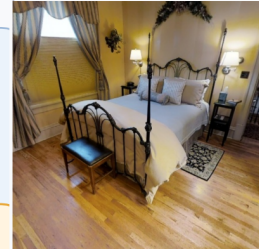
#### 3 Turn 3

##### Thinking:

I can now see a bed with decorative pillows and a light blanket in the projected view! The object is in the central region. I should zoom into that area to get a clearer view of the target object. By narrowing the field of view, I can observe more details and determine the precise location. Adjusting to azimuth  $157.7^\circ$  and elevation  $-24.2^\circ$  with FOV  $75.8^\circ$ .

**Tool call:** `rotate_and_project_panorama(azimuth=157.7°, elevation=-24.2°, fov_degrees=75.8°)`

Projected view (az=157.7°, el=-24.2°, fov=75.8°)



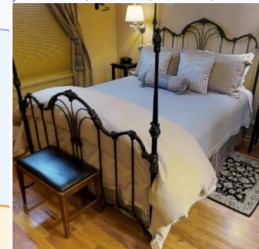
#### 4 Turn 4

##### Thinking:

Found a bed with decorative pillows and a light blanket! It appears in the central region in the current view. Let me magnify this region to see the object more clearly. A closer look will help me pinpoint the exact coordinates. Rotating to azimuth  $157.7^\circ$  and elevation  $-24.2^\circ$  with FOV  $51.6^\circ$ .

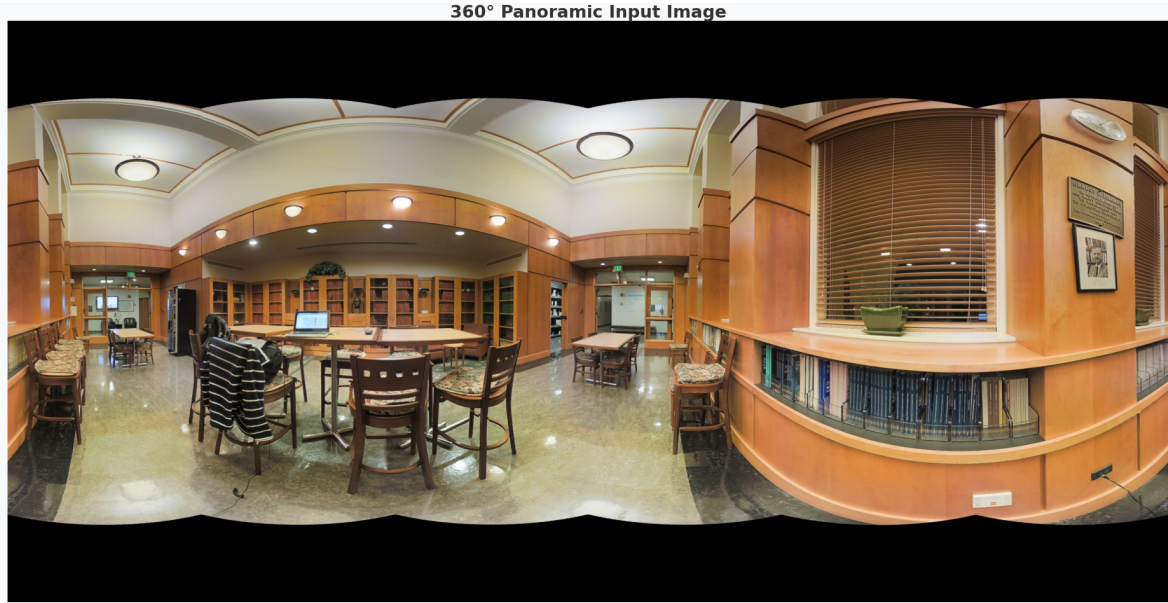
**Tool call:** `rotate_and_project_panorama(azimuth=157.7°, elevation=-24.2°, fov_degrees=51.6°)`

Projected view (az=157.7°, el=-24.2°, fov=51.6°)



**Answer:** The a bed with decorative pillows and a light blanket is located at: - Azimuth:  $157.7^\circ$  - Elevation:  $-24.2^\circ$

Figure 5: A training data sample from Matterport3D (Chang et al., 2017)



**Q:** This is a 360-degree panoramic image. Where is a black vending machine located? Please provide the spherical coordinates (azimuth and elevation in degrees).

**1 Turn 1**

**Thinking:**  
This is a full 360-degree panoramic view. My task is to locate a black vending machine. Based on visual cues and scene context, I estimate the object might be at azimuth  $-101^\circ$  and elevation  $-3^\circ$ . Let me rotate to verify this estimate.

**Tool call:** `rotate_and_project_panorama(azimuth=-100.6°, elevation=-2.6°, fov_degrees=100.0°)`

Projected view (az=-100.6°, el=-2.6°, fov=100.0°)

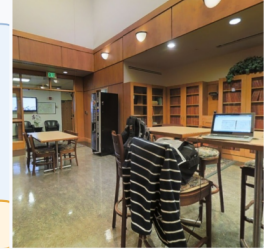


**2 Turn 2**

**Thinking:**  
I've located a black vending machine in this view, positioned centrally positioned but a bit to the left. To better examine the target and determine its precise spherical coordinates, I need to enlarge this area. Zooming in to azimuth  $-114.9^\circ$  and elevation  $-2.8^\circ$  with FOV  $73.3^\circ$ .

**Tool call:** `rotate_and_project_panorama(azimuth=-114.9°, elevation=-2.8°, fov_degrees=73.3°)`

Projected view (az=-114.9°, el=-2.8°, fov=73.3°)

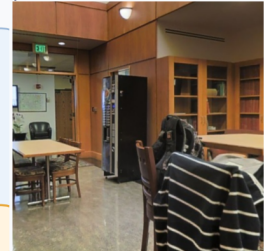


**3 Turn 3**

**Thinking:**  
A black vending machine is visible centrally positioned but a bit to the left in the current projection. I should enlarge this region to observe the target more clearly and determine its coordinates precisely. Zooming in to azimuth  $-123.4^\circ$  and elevation  $-2.9^\circ$  with FOV  $46.7^\circ$ .

**Tool call:** `rotate_and_project_panorama(azimuth=-123.4°, elevation=-2.9°, fov_degrees=46.7°)`

Projected view (az=-123.4°, el=-2.9°, fov=46.7°)

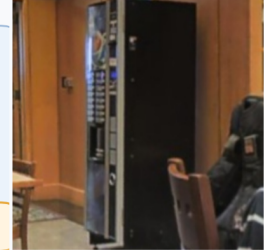


**4 Turn 4**

**Thinking:**  
I've located a black vending machine in this view, positioned right at the center of the view. To better examine the target and determine its precise spherical coordinates, I need to enlarge this area. Zooming in to azimuth  $-126.3^\circ$  and elevation  $-2.9^\circ$  with FOV  $20.0^\circ$ .

**Tool call:** `rotate_and_project_panorama(azimuth=-126.3°, elevation=-2.9°, fov_degrees=20.0°)`

Projected view (az=-126.3°, el=-2.9°, fov=20.0°)



**Answer:** The a black vending machine is located at: - Azimuth:  $-126.3^\circ$  - Elevation:  $-2.9^\circ$

Figure 6: A training data sample from 2D-3D-S (Armeni et al., 2017)

360° Panoramic Input Image



Q: This is a 360-degree panoramic image. Locate a decorative floral arrangement in a vase and specify its angular coordinates in degrees.

1 Turn 1

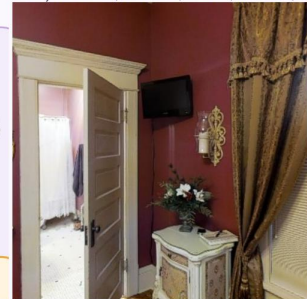
Thinking:

The target object, a decorative floral arrangement in a vase, is visible in the panoramic view. It's located on the left side of the scene. To accurately determine its position, I will zoom in by adjusting the view to center on this object and narrow the field of view. This will allow me to precisely identify its azimuth and elevation angles. First, I'll rotate the view to center on the decorative floral arrangement and then adjust the field of view to focus on it.



Tool call: rotate\_and\_project\_panorama(azimuth=-100.0°, elevation=-1.0°, fov\_degrees=63.0°)

Projected view (az=-100.0°, el=-1.0°, fov=63.0°)



2 Turn 2

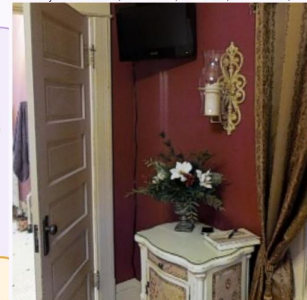
Thinking:

The decorative floral arrangement in a vase is visible in the lower left portion of the frame. To accurately determine its position, I will zoom in further by adjusting the view to center on this object and narrowing the field of view. This will allow me to precisely identify its azimuth and elevation angles. Now, I'll rotate the view to center on the decorative floral arrangement and then adjust the field of view to focus on it.



Tool call: rotate\_and\_project\_panorama(azimuth=-98.0°, elevation=-7.0°, fov\_degrees=44.0°)

Projected view (az=-98.0°, el=-7.0°, fov=44.0°)



3 Turn 3

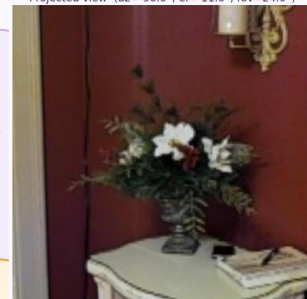
Thinking:

The decorative floral arrangement in a vase is now visible in the lower center of the frame. To accurately determine its position, I will zoom in further by adjusting the view to center on this object and narrowing the field of view. This will allow me to precisely identify its azimuth and elevation angles. Now, I'll rotate the view to center on the decorative floral arrangement and then adjust the field of view to focus on it.



Tool call: rotate\_and\_project\_panorama(azimuth=-96.0°, elevation=-11.0°, fov\_degrees=24.0°)

Projected view (az=-96.0°, el=-11.0°, fov=24.0°)




Answer: The a decorative floral arrangement in a vase is located at: - Azimuth: -96.0° - Elevation: -11.0°

GT: az=-95.7°, el=-11.3°

Pred: az=-96.0°, el=-11.0° dist=0.43° ✓

Figure 7: A inference case of EAGLE-360


**360° Panoramic Input Image**



**Q:** This is a 360-degree panoramic image. I need to locate a flat-screen television in a red bounding box. Please give me the azimuth and elevation in degrees.

**1 Turn 1**


**Thinking:**  
The target object, a flat-screen television, is visible in the panoramic view. It's located on the left side of the scene. To accurately determine its position, I will zoom in by adjusting the view to center on this television and narrow the field of view. This will allow me to precisely identify its azimuth and elevation angles. First, I'll rotate the view to center on the television and then adjust the field of view to focus on it.



**Tool call:** rotate\_and\_project\_panorama(azimuth=-70.0°, elevation=0.0°, fov\_degrees=63.0°)

**2 Turn 2**


**Thinking:**  
The flat-screen television is visible in the upper left portion of the frame. To accurately determine its position, I will zoom in by adjusting the view to center on this television and narrowing the field of view. This will allow me to precisely identify its azimuth and elevation angles. Now, I'll rotate the view to center on the television and then adjust the field of view to focus on it.



**Tool call:** rotate\_and\_project\_panorama(azimuth=-78.0°, elevation=3.0°, fov\_degrees=44.0°)

**3 Turn 3**


**Thinking:**  
The flat-screen television is now clearly centered in the frame. The field of view has been narrowed, which allows me to observe the object's details more precisely. To accurately determine its position, I will zoom in further by adjusting the view to center on the television and reducing the field of view to just encompass it. This will ensure that the azimuth and elevation angles are measured with high precision. Now, I'll submit the final answer.




**Tool call:** rotate\_and\_project\_panorama(azimuth=-82.0°, elevation=5.0°, fov\_degrees=24.0°)

**Answer:** The a flat-screen television is located at: - Azimuth: -82.0° - Elevation: 5.0°  
GT: az=-80.3°, el=5.0°  
Pred: az=-82.0°, el=5.0° dist=1.67° ✓

Projected view (az=-70.0°, el=0.0°, fov=63.0°)



Projected view (az=-78.0°, el=3.0°, fov=44.0°)



Projected view (az=-82.0°, el=5.0°, fov=24.0°)

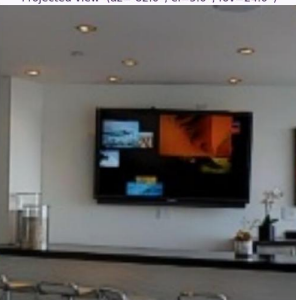


Figure 8: A inference case of EAGLE-360

### 360° Panoramic Input Image



**Q:** This is a 360-degree panoramic image. Could you find a black leather handbag and provide its spherical coordinates in degrees?

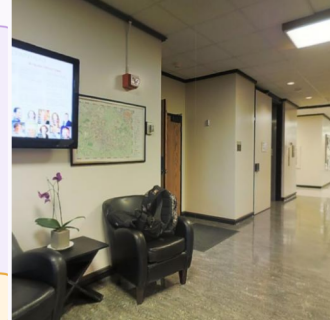
#### 1 Turn 1

##### Thinking:

The target object, a black leather handbag, is visible in the panoramic view. It's located on the right side of the scene, resting on a black leather armchair. To accurately determine its position, I will zoom in by adjusting the view to center on this object and narrow the field of view. This will allow me to precisely identify its azimuth and elevation angles. First, I'll rotate the view to center on the black leather handbag and then adjust the field of view to focus on it.



Projected view (az=40.0°, el=-1.0°, fov=63.0°)



**Tool call:** rotate\_and\_project\_panorama(azimuth=40.0°, elevation=-1.0°, fov\_degrees=63.0°)

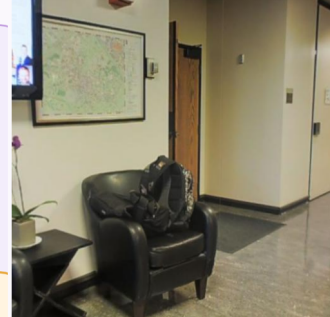
#### 2 Turn 2

##### Thinking:

The black leather handbag is visible in the lower center of the frame, resting on a black leather armchair. To accurately determine its position, I will zoom in by adjusting the view to center on this object and narrowing the field of view. This will allow me to precisely identify its azimuth and elevation angles. Now, I'll rotate the view to center on the black leather handbag and then adjust the field of view to focus on it.



Projected view (az=38.0°, el=-7.0°, fov=44.0°)



**Tool call:** rotate\_and\_project\_panorama(azimuth=38.0°, elevation=-7.0°, fov\_degrees=44.0°)

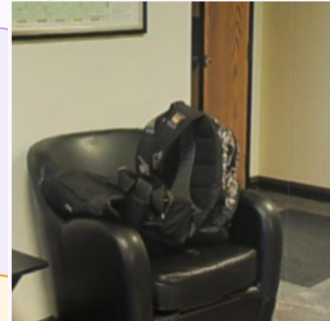
#### 3 Turn 3

##### Thinking:

The black leather handbag is now visible in the lower left portion of the frame, resting on a black leather armchair. To accurately determine its position, I will zoom in by adjusting the view to center on this object and narrowing the field of view. This will allow me to precisely identify its azimuth and elevation angles. Now, I'll rotate the view to center on the black leather handbag and then adjust the field of view to focus on it.



Projected view (az=36.0°, el=-11.0°, fov=24.0°)



**Tool call:** rotate\_and\_project\_panorama(azimuth=36.0°, elevation=-11.0°, fov\_degrees=24.0°)

**Answer:** The a black leather handbag is located at: - Azimuth: 36.0° - Elevation: -11.0°

GT: az=36.0°, el=-11.9°

**Pred:** az=36.0°, el=-11.0° dist=0.90° ✓

Figure 9: A inference case of EAGLE-360